1 **The Arctic picoeukaryote *Micromonas pusilla* benefits**

2 **synergistically from warming and ocean acidification**

4 Clara J. M. Hoppe[1,2]*, Clara M. Flintrop[1,3] and Björn Rost[1]

6 [1] Marine Biogeosciences, Alfred Wegener Institute – Helmholtz Centre for Polar and Marine

7 Research, 27570 Bremerhaven, Germany

8 [2] Norwegian Polar Institute, 9296 Tromsø, Norway

9 [3] MARUM, 28359 Bremen, Germany

11 *Correspondence to: Clara J. M. Hoppe (Clara.Hoppe@awi.de)

15 **Abstract**

16 In the Arctic Ocean, climate change effects such as warming and ocean acidification (OA) are

17 manifesting faster than in other regions. Yet, we are lacking a mechanistic understanding of the

18 interactive effects of these drivers on Arctic primary producers. In the current study, one of the

19 most abundant species of the Arctic Ocean, the prasinophyte *Micromonas pusilla*, was exposed

20 to a range of different $pCO_2$ levels at two temperatures representing realistic current and future

21 scenarios for nutrient-replete conditions. We observed that warming and OA synergistically

22 increased growth rates at intermediate to high $pCO_2$ levels. Furthermore, elevated temperatures

23 shifted the $pCO_2$-optimum of biomass production to higher levels. Based on changes in cellular

24 composition and photophysiology, we hypothesise that the observed synergies can be explained

25 by beneficial effects of warming on carbon fixation in combination with facilitated carbon

26 acquisition under OA. Our findings help to understand the higher abundances of picoeukaryotes

27 such as *M. pusilla* under OA, as has been observed in many mesocosm studies.

## 1 Introduction

With the progress in using molecular tools to describe marine biodiversity in the past decades, the scientific community has become increasingly aware of the underestimated importance of picoeukaryotes, for both primary and export production of the world's oceans (Richardson and Jackson, 2007; Worden and Not, 2008). Larger phytoplankton such as diatoms are efficient vectors for carbon export due to aggregate formation and ingestion by large zooplankton leading to the production of fast-settling faecal pellets (Sherr et al., 2003). In contrast, picoeukaryotes are mainly grazed by smaller heterotrophic protists such as ciliates, which have a low carbon retention, excrete relatively more dissolved material, and thus fuel recycled production (Sherr and Sherr, 2002). Hence, changes in the relative abundance of pico- and nanoeukaryotes can have large implications for food webs and biogeochemistry (Worden et al., 2015).

Picoeukaryotes tend to dominate low nutrient environments, which is often attributed to their high surface:volume ratios and mixotrophic capacities (Raven, 1998; McKie-Krisberg and Sanders, 2014). The low nutrient concentrations in the Arctic surface ocean, for example, cause picoeukaryotes to be particularly successful in this region. In fact, the globally occurring prasinophyte *Micromonas pusilla* is considered the most abundant species in the Arctic ocean (Šlapeta et al., 2006; Lovejoy et al., 2007; Marquardt et al., 2016). In this environment, strong stratification causes low nutrient concentrations throughout the summer and autumn months (Tremblay et al., 2015), and the occurrence of the polar night requires organisms to either form resting stages or to have heterotrophic capacities (Tremblay et al., 2009; Lovejoy, 2014; Berge et al., 2015; Vader et al., 2015).

Climate change effects manifest faster in the Arctic than anywhere else on the planet (Stocker, 2014). In this region, for example, temperatures are rising more than twice as fast as at the rest of the globe (Miller et al., 2010). The concurrent rapid reduction in ice cover allows for more light penetration and longer growing seasons, while increased stratification due to ice melt and warming constrain nutrient supply to surface waters, both of which will change the dynamics of primary production (Arrigo et al., 2008; Wassmann and Reigstad, 2011). Ocean acidification (OA) is also especially pronounced in the Arctic Ocean, because low temperatures and alkalinity make the system sensitive to anthropogenic $CO_2$ loading (AMAP, 2013; Qi et al., 2017). Picoeukaryotes such as *M. pusilla* may benefit from these changes and are considered potential winners of climate change. In the Canadian Arctic, for example, picoeukaryote abundances are increasing as surface waters get warmer, fresher and more oligotrophic (Li et al., 2009). Regarding OA effects, the majority of studies on natural phytoplankton assemblages

62     have shown picoeukaryotes, particularly *M. pusilla*, to increase in relative abundance with

63     increasing $pCO_2$ levels (Engel et al., 2008; Meakin and Wyman, 2011; Newbold et al., 2012;

64     Brussaard et al., 2013; Hussherr et al. 2017; Schulz et al., 2017). Despite the evident sensitivity

65     of *M. pusilla* to changes in $pCO_2$ levels, a detailed assessment of the OA effects, their

66     interaction with warming as well as the underlying mechanisms in this important species is still

67     missing.

68          Like all photosynthetic organisms, cells of *M. pusilla* need to maintain a balance

69     between energy sources (i.e. light harvesting by the photosynthetic apparatus) and sinks (most

70     importantly carbon fixation in the Calvin cycle) to prevent harmful levels of excitation pressure

71     on the photosynthetic electron transport chain (Behrenfeld et al., 2008). Light harvesting and

72     electron transport in the photosystems are largely independent of changes in temperature and

73     $pCO_2$ (Mock and Hoch, 2005; Hoppe et al., 2015), but the impact of these drivers on energy

74     sinks can potentially affect the energy balance of the cell: The beneficial effects of elevated

75     $pCO_2$ observed in phytoplankton are thought to be caused by increased diffusive $CO_2$ supply,

76     reduced $CO_2$ leakage, or by lowered costs to operate their $CO_2$ concentrating mechanisms (Rost

77     et al., 2008; Bach et al., 2013). Elevated temperatures, on the other hand, can change enzyme

78     kinetics including those involved in the Calvin cycle, thus leading to a larger sink of excitation

79     energy (Maxwell et al., 1994; Toseland et al., 2013). Hence, both ocean warming and

80     acidification potentially increase the efficiency of photosynthesis and biomass production, at

81     least up to the organisms' respective optimum levels. Above these levels, temperatures and

82     proton concentrations start to disrupt enzymatic processes, increase the investment into pH

83     homeostasis, and impair the delicate regulation of cellular processes (Levitt, 1980; Taylor et

84     al., 2001; Flynn et al., 2012). Thus, the complex balance between beneficial and detrimental

85     effects will determine whether the combination of warming and OA will synergistically

86     promote or deteriorate phytoplankton growth and biomass build-up.

87          In the current study, we aim to investigate the responses of an Arctic *M. pusilla* strain

88     to warming and OA. To this end, *M. pusilla* was grown at four $pCO_2$ levels ranging from

89     preindustrial to future scenarios (180-1400 µatm) under 2°C and 6°C, which represent the

90     magnitude of the projected future temperature increase in this region (Collins et al., 2013), but

91     also the current spring and summer temperatures in the environment where the strain was

92     isolated (Hegseth et al., in press).

## 2 Material & Methods

### 2.1 Culture conditions

Monoclonal cultures of the picoeukaryote *Micromonas pusilla* (Butcher) I. Manton & M. Parke (isolated in 2014 by K. Wolf in Kongsfjorden, Svalbard, 79°N; local temperature range -1.5 to 8°C) taxonomic identification confirmed by rDNA sequencing of SSU, LSU and ITS sequences) were grown in 1-L glass bottles in semi-continuous dilute-batch cultures (max 129,000 cells mL$^{-1}$; diluted every 3-4 days) under constant irradiances of $150 \pm 26$ µmol photons m$^{-2}$ s$^{-1}$. Media consisted of 0.2 µm sterile-filtered Arctic seawater with a salinity of 32.7 enriched with macronutrients, trace metals and vitamins according to F/2$_R$ medium (Guillard and Ryther, 1962). Light intensities were provided by daylight lamps (Philips Master TL-D 18W; emission peaks at wavelength of 440, 560 and 635 nm), adjusted by neutral density screens and monitored using a LI-1400 data logger (Li-Cor) equipped with a $4\pi$-sensor (Walz). Cells were growing at four different $CO_2$ partial pressures (pCO$_2$; 180, 380, 1000, and 1400 µatm) and two temperatures ($2.2 \pm 0.3$°C and $6.3 \pm 0.2$°C). Cultures were acclimated to these conditions for at least 7 generations prior to sampling.

Different pCO$_2$ conditions were achieved by aeration of the incubation bottles with air of the respective pCO$_2$ levels delivered through sterile 0.2-µm air-filters (Midisart 2000, Sartorius stedim) for 24 h prior to inoculation. Gas mixtures were generated using a gas flow controller (CGM 2000 MCZ Umwelttechnik), in which $CO_2$-free air (<1 ppmv $CO_2$; Dominick Hunter) was mixed with pure $CO_2$ (Air Liquide Deutschland). The pCO$_2$ levels in the gas mixtures were regularly monitored with a non-dispersive infrared analyzer system (LI6252, LI-COR Biosciences), calibrated with $CO_2$-free air and purchased gas mixtures of $150 \pm 10$ and $1000 \pm 20$ ppmv $CO_2$ (Air Liquide Deutschland).

### 2.2 Carbonate chemistry

Samples for total alkalinity (A$_T$) were filtered through 0.7-µm glass fibre filters (GF/F, Whatman) and stored in borosilicate bottles at 3°C. A$_T$ was estimated from duplicate potentiometric titration (Brewer et al., 1986) using a TitroLine alpha plus (Schott Instruments). A$_T$ values were corrected for systematic errors based on measurements of certified reference materials (CRMs provided by Prof. A. Dickson, Scripps, USA; batch #111; reproducibility $\pm 5$ µmol kg$^{-1}$). Total dissolved inorganic carbon (C$_T$) samples were filtered through 0.2-µm cellulose-acetate filters (Sartorius stedim) and stored in gas-tight borosilicate bottles at 3°C. C$_T$ was measured colorimetrically in triplicates with a QuAAtro autoanalyzer (Seal; Stoll et al.

127 2001). The analyser was calibrated with $NaHCO_3$ solutions (with a salinity of 35, achieved by
128 addition of NaCl) to achieve concentrations ranging from 1800 to 2300 µmol $C_T$ kg$^{-1}$. CRMs
129 were used for corrections of errors in instrument performance such as baseline drifts
130 (reproducibility ±8 µmol kg$^{-1}$). Seawater pH$_{total}$ was measured potentiometrically with a two-
131 point calibrated glass reference electrode (IOline, Schott Instruments). An internal TRIS-based
132 reference standard (Dickson et al., 2007) was used to correct for variability on electrode
133 performance (reproducibility ±0.015 pH units). Following recommendations by Hoppe et al.
134 (2012), seawater carbonate chemistry including pCO$_2$ was calculated from $A_T$ and pH using
135 CO$_2$SYS (Pierrot et al., 2006). The dissociation constants of carbonic acid of Mehrbach et al.
136 (1973), as refitted by Dickson and Millero (1987), were used for calculations. Dissociation
137 constants for KHSO$_4$ were taken from Dickson (1990).

138

## 2.3 Growth, elemental composition and production rates

140 Samples for cell counts were fixed with glutaraldehyde (0.5% final concentration). After gentle
141 mixing, samples were stored at room temperature in the dark for 15 min, and subsequently
142 frozen in liquid nitrogen and stored at -80°C. Prior to analysis, samples were thawed on ice and
143 mixed thoroughly. After addition of 10 µL SybrGreen working solution (dissolved in DMSO)
144 and 10 µL YG beads working solution (1µm-Flouresbrite calibration beads grade YG,
145 Polyscience), samples were counted on an Accuri C6 flow cytometer (BD Biosciences)
146 equipped with a blue solid-state laser (488 nm excitation wavelength) run on medium fluidics
147 settings (35 µL min$^{-1}$; 16 µm core size) with a limit of 50,000 events or 250 µL. Analysis was
148 performed based on red (FL3 channel, >670 nm) and green (FL1 channel, 533 ± 30 nm)
149 fluorescence, as well as sideward and forward light scattering. Specific growth rates constants
150 (µ) were determined from exponential fits of cell counts over 4 consecutive days.

151 Particulate organic carbon (POC) and nitrogen (PON) were measured after filtration
152 onto precombusted (15h, 500 °C) GF/F filters (Whatman) and stored at -20 °C. and dried for
153 at least 12 h at 60 °C prior to sample preparation. Analysis was performed using a CHNS-O
154 elemental analyser (Euro EA 3000, HEKAtech). Contents of POC and PON were corrected for
155 blank measurements and normalised to filtered volume and cell densities to yield cellular
156 quotas. Production rates of POC were calculated by multiplying the cellular quota with the
157 division rate constant $k$ of the respective incubation. Samples for determination of chlorophyll
158 a (Chl $a$) were filtered onto GF/F filters (Whatman), immediately placed into liquid nitrogen
159 and stored at -80°C until analysis. Chl $a$ was subsequently extracted in 8 mL 90% acetone at

160  4°C over night. Chl *a* concentrations were determined on a fluorometer (TD-700, Turner

161  Designs), using an acidification step (1M HCl) to determine phaeopigments (Knap et al., 1996).

162

163  **2.4 Variable Chl *a* fluorescence**

164  Photophysiological characteristics, based on photosystem II (PSII) variable Chl *a* fluorescence,

165  were measured using a fast repetition rate fluorometer (FRRf; FastOcean PTX, Chelsea

166  Technologies) in combination with a FastAct Laboratory system (Chelsea Technologies). The

167  excitation wavelength of the fluorometer's light-emitting diodes (LEDs) was 450 nm, and the

168  applied light intensity was 21587 µmol photons $m^{-2}$ $s^{-1}$. The FRRf was used in single turnover

169  mode, with a saturation phase comprising 100 flashlets on a 2 µs pitch and a relaxation phase

170  comprising 40 flashlets on a 50 µs pitch. Measurements from all replicates (n=3) were

171  conducted in a temperature-controlled chamber (±0.2°C) at the respective treatment

172  temperature.

173  After subtraction of a blank value, the minimum ($F_0$ and $F_0'$ for light-and dark-

174  acclimated measurements, respectively) and maximum Chl *a* fluorescence ($F_m$, and $F_m'$ for

175  light-and dark-acclimated measurements, respectively) were estimated from iterative

176  algorithms for induction (Kolber et al., 1998) and relaxation phase (Oxborough, 2012) after 15

177  min of dark acclimation, which was sufficient to achieve a dark-acclimated state (data not

178  shown). All fluorescence parameters were calculated by standard equations (Genty et al., 1989;

179  Maxwell and Johnson, 2000). Maximum quantum yields of PSII (apparent PSII photochemical

180  quantum efficiency; $F_v/F_m$) were calculated as

181      $$F_v/F_m = (F_m - F_0)/F_m \tag{1}$$

182  Fluorescence based photosynthesis-irradiance curves (PI) were conducted at six irradiances (I)

183  between 33 and 672 µmol photons $m^{-2}$ $s^{-1}$, with an acclimation time of 10 min per light step.

184  Electron transfer rate through PSII (ETR [mol $e^-$ (mol RCII)$^{-1}$ $s^{-1}$]) for each light step was

185  calculated as:

186      $$ETR = ((F_m' - F_0')/F_m') * I \tag{2}$$

187  Following the suggestion by Silsbe and Kromkamp (2012), the light-use efficiency (α [mol $e^-$

188  $m^2$ (mol RCII)$^{-1}$ (mol photons)$^{-1}$]) and the maximum electron transfer rates per RCII ($ETR_{max}$

189  [mol $e^-$ (mol RCII)$^{-1}$ $s^{-1}$]) were estimated by fitting the data to the model by (Webb et al., 1974):

190      $$ETR = ETR_{max} * [1 - e^{(-(\alpha*I)/ETR_{max})}] \tag{3}$$

191  The light saturation index ($E_k$ [µmol photons $m^{-2}$ $s^{-1}$]) was then calculated as $ETR_{max}/\alpha$.

192  Maximum non-photochemical quenching of Chl *a* fluorescence (NPQ) at irradiances of 672

193 μmol photons $m^{-2}$ $s^{-1}$ (i.e. the highest irradiance step of the PI curve) were calculated using the

194 normalized Stern-Volmer coefficient, also termed NSV, as described in McKew et al. (2013):

195 $\quad (F_q'/F_v')-1 = F_0'/F_v'$ $\qquad\qquad\qquad\qquad\qquad\qquad\qquad\qquad$ (4)

196 where $F_q'$ is the differences between measured and maximal fluorescence (Suggett et al., 2010).

197 $F_0'$ was measured after each light step (with a duration of 90 s).

198

199 **2.5 Statistics**

200 All data is given as the mean of three biological replicates with ± one standard deviation. To

201 test for significant differences between the treatments, two-way analyses of variance (ANOVA)

202 with additional normality (Kolmogorov-Smirnov) and Post Hoc (Holm-Sidak) tests were

203 performed. The significance level was set to 0.05. Statistical analyses were performed with the

204 program SigmaPlot (SysStat Software Inc, Version 12.5).

205

## 3 Results

### 3.1 Carbonate Chemistry

Regular dilution of cultures with pre-aerated seawater medium kept carbonate chemistry stable over the course of the experiment. More specifically, in each bottle the drift in $A_T$ and $C_T$ compared to initial values was $\leq 3\%$ and $\leq 4\%$, respectively (data not shown). Final carbonate chemistry in the 2°C treatments yielded $pCO_2$ levels of $197 \pm 3$, $323 \pm 12$, $959 \pm 22$ and $1380 \pm 53$ µatm (Table 1). In the 6°C treatments, $pCO_2$ levels were $198 \pm 6$, $394 \pm 10$, $1036 \pm 31$ and $1449 \pm 18$ µatm. Please note that the same $pCO_2$ level translates into differing dissolved $CO_2$ concentrations at different temperatures due to the temperature dependency of the carbonate system. Specifically, the treatment $pCO_2$ values translated into up to 13% lower dissolved $CO_2$ concentrations in the 6°C compared to the 2°C treatment (Table 1; cf. Figure SI1). Concurrently, the $pCO_2$ levels at 2°C corresponded to $pH_{total}$ values of $8.30 \pm 0.01$, $8.11 \pm 0.01$, $7.68 \pm 0.01$ and $7.52 \pm 0.02$, respectively. In the 6°C treatment, $pH_{total}$ values of the four $pCO_2$ treatments were $8.30 \pm 0.01$, $8.04 \pm 0.01$, $7.65 \pm 0.01$ and $7.52 \pm 0.01$, respectively.

### 3.2 Growth and biomass build-up

Growth rates constants of exponentially growing *M. pusilla* cultures were significantly affected by the applied treatments (Figure 1, Table 2, SI1). Depending on the $pCO_2$ level, temperature increased growth by 20 to 60% with an average of $0.80$ d$^{-1}$ under low and $1.10$ d$^{-1}$ under high temperature conditions (two-way ANOVA, F = 328, p <0.001). Overall, there was also a positive $pCO_2$ effect on growth (two-way ANOVA, F = 9, p = 0.001), even though no linear trends with either $pCO_2$ or $[CO_2]$ were observed (Figure 1, SI1). The observed $pCO_2$ responses also differed between temperature levels, indicating a significant interaction between both drivers (two-way ANOVA, F = 12, p <0.001): Under low temperature, growth increased significantly from 180 to 380 µatm $pCO_2$ (post-hoc, t = 3.1, p = 0.04), while there was a declining, yet insignificant trend in growth with further increases in $pCO_2$. Under high temperature, growth was significantly higher under 1000 compared to lower (180 µatm; post-hoc, t = 5.6, p <0.001) and higher $pCO_2$ levels (1400 µatm; post-hoc, t = 5.9, p <0.001). Thus, warming shifted the optimum range for growth to higher $pCO_2$ levels (Figure 1A).

This trend was also observed in terms of POC production rates (Figure 1B, Table 2), with significant effects of temperature (Table SI1; two-way ANOVA, F = 356, p <0.001), $pCO_2$ (two-way ANOVA, F = 7, p = 0.003), and their interaction (two-way ANOVA, F = 29, p <0.001). At low temperatures, higher production rates were observed at 180 and 380 µatm

240    compared to those at 1000 and 1400 µatm $pCO_2$ (post-hoc tests, t = 3.5, p = 0.016 and t = 3.0,
241    p = 0.046, respectively). At high temperatures, POC production rates were significantly higher
242    at 1000 µatm than at all other $pCO_2$ levels (post-hoc tests, e.g. t = 9.1, p <0.001 for 380 vs.
243    1000 µatm and t = 7.4, p <0.001 for 1000 vs. 1400 µatm), again indicating an upward shift in
244    the $pCO_2$ optimum with warming.
245

**3.3 Cellular composition**

247    Overall, POC quota (Figure 2 a, Table 2, Table SI1) were significantly higher under elevated
248    compared to low temperature (two-way ANOVA, F = 24, p <0.001), but no overarching trend
249    with $pCO_2$ was observed. Under low temperature, cells had significantly higher POC quota at
250    low $pCO_2$ levels (180 and 380 µatm) compared to high $pCO_2$ levels (1000 and 1400 µatm; all
251    four post-hoc tests significant, e.g. 380 vs 1000µatm: t = 2.8, p = 0.033). This trend reversed
252    under high temperature, where POC quota were highest under 1000 and 1400 µatm (post-hoc
253    test, t = 3.5, p = 0.024). Thus, temperature and $pCO_2$ levels exhibited a significant interactive
254    effect on POC quota (two-way ANOVA, F = 10, p <0.001).
255        Similar trends were observed in terms of cellular PON quota (Figure 2 b, Table 2, Table
256    SI1), where temperature (two-way ANOVA, F = 5, p = 0.045) and its interaction with $pCO_2$
257    (two-way ANOVA, F = 10, p <0.001) significantly affected the results. Here, opposing $pCO_2$
258    effects under different temperatures were more subtle, with PON quota under low temperatures
259    only being significantly decreased between 380 and 1400 µatm (post-hoc test, t = 3.3, p =
260    0.027), while under high temperature PON quota significantly increased from 180 and 380 to
261    1000 µatm $pCO_2$ (post-hoc tests, t = 3.7, p = 0.012 and t = 2.8, p = 0.028, respectively).
262        Regarding cellular Chl *a* quota, there were no significant effects of temperature or $pCO_2$
263    alone (Figure 2 c, Table 2, Table SI1), but a significant interaction between the two drivers
264    (two-way ANOVA, F = 18, p <0.001): Under low temperature, Chl *a* quota decreased from low
265    (180 µatm) to high $pCO_2$ levels (1000 and 1400 µatm; post-hoc tests, t = 5.0, p <0.001 and t =
266    3.9, p = 0.006, respectively). Under high temperature, the opposite trend was observed, where
267    Chl *a* quota increased from low (180 and 380 µatm) to high $pCO_2$ levels (1000 and 1400 µatm;
268    all four post-hoc tests significant, e.g. 380 vs 1000µatm: t = 3.0, p = 0.027).
269        Molar C:N ratios of the biomass (Table 2, Table SI1) increased with temperature (two-
270    way ANOVA, F = 14, p = 0.002), yet this overall difference was mainly driven by results at
271    low $pCO_2$ levels (180 and 380 µatm; post-hoc tests, t = 2.7, p = 0.017 and t = 3.5, p = 0.003,
272    respectively). By itself, $pCO_2$ did not significantly affect C:N ratios.
273        The ratios of C:Chl *a* (Figure 2 d, Table 2, Table SI1) were elevated under high

274    compared to low temperature conditions (two-way ANOVA, F = 14, p = 0.002), an effect that

275    was most pronounced at $pCO_2$ levels of 180 µatm (post-hoc test, t = 5.5, p <0.001). While there

276    was no effect of $pCO_2$ on C:Chl $a$ at low temperature, C:Chl $a$ decreased with increasing $pCO_2$

277    at high temperature (two-way ANOVA, interaction term, F = 6, p = 0.007; 180 vs. 1400 µatm

278    at 6°C post-hoc test, t = 3.9, p = 0.008).

279

280    **3.4 Chl $a$ fluorescence-based photophysiology**

281    The effects of the applied treatments on photophysiology were studied by means of FRRf,

282    which investigates photochemistry at photosystem II (PSII). No effects of the applied

283    treatments were observed in most parameters investigated (Table 3, SI1). This was true for the

284    dark-acclimated quantum yield efficiency of PSII ($F_v/F_m$), which was similar in all treatments

285    with values of 0.45 ±0.06, as well as for absorption cross section of PSII light harvesting ($\sigma_{PSII}$).

286            Furthermore, the fitted parameters of FRRf-based PI curves ($\alpha$, $ETR_{max}$ and $E_K$) were

287    independent of the experimental treatments (Table 3, SI1). In contrast, the rate constant of the

288    reopening of PSII reaction centres ($\tau_{ES}$; Table 3, SI1) was slightly yet significantly smaller

289    under high temperatures (two-way ANOVA, F = 6, p = 0.029), even though this overall

290    response also depended on the applied $pCO_2$ levels (two-way ANOVA, interaction term, F = 4,

291    p = 0.033).

292            Maximum non-photochemical quenching ($NPQ_{max}$; Table 3, SI1) increased

293    significantly with $pCO_2$ (Table SI1; two-way ANOVA, F = 0, p = 0.002) while temperature had

294    no effect. Post-hoc tests revealed that this response was mainly driven by high $NPQ_{max}$ values

295    at 1000 µatm, which were significantly higher than in any other $pCO_2$ treatment (e.g. t = 4.1, p

296    = 0.006 for 380 vs. 1000 µatm and t = 3.1, p = 0.030 for 1000 vs. 1400 µatm).

**4 Discussion**

**4.1 *Micromonas pusilla* benefits from warming**

We observed a strong stimulation of growth rates and biomass build-up with increasing temperature (Figure 1, Table 2). Even though the isolate stems from 1.8°C water temperature, the beneficial effects of warming from 2°C to 6°C are not surprising: *M. pusilla* is known to dominate Arctic phytoplankton assemblages in the summer and autumn situations (Lovejoy et al., 2007; Marquardt et al., 2016) when surface temperatures of 6°C or more can be reached (Hegseth et al., in press). Our results are also in line with mesocosm experiments that indicate stimulatory effects of warming on picoplankton abundances (Daufresne et al., 2009; Sommer et al., 2015) as well as with the temperature optimum of 6-8°C observed for another Arctic strain of *M. pusilla* (Lovejoy et al., 2007).

Below the temperature optimum of a cell, warming causes an acceleration of the entire metabolism, as enzymatic reactions run faster under these conditions (Eppley, 1972; Brown et al., 2004). In this study, warming caused higher growth rates, POC quotas and biomass production (Figure 2, Tables 2, SI1), indicating that particularly the fixation and storage of carbon was facilitated by increasing temperature. Electron transport processes, on the other hand, were largely independent of temperature (Tables 3, SI1). Thus, temperature affected the balance between electron transport ('light reaction') and carbon fixation in the Calvin cycle ('dark reactions'). Especially under relatively low temperatures, as investigated here, warming can decrease the excitation pressure on the electron transport chain of the photosystems by increasing the temperature-limited turnover rates of enzyme reaction such as RuBisCO (Mock and Hoch, 2005). Thus, cells grown under low temperature need to invest relatively more energy into biosynthesis than into photochemistry compared to cells grown under high temperature (Toseland et al., 2013). While it has been shown that Antarctic diatoms can compensate for slow RuBisCO kinetics by increasing the expression of this enzyme (Young et al., 2014), it is unknown whether such acclimation responses also occur in prasinophytes. Regarding the C:Chl *a* ratio, this can be taken as an in indicator on how much resources the cell retains as carbon biomass (e.g. structural and storage compounds) relative to how much is invested into its light harvesting capacities (Halsey and Jones, 2015). In this study, the strong temperature-dependent increase in C:Chl *a* (Figure 2, Table SI1) under potentially limiting $pCO_2$ levels of 180 µatm suggests that under warming, the balance between light harvesting and carbon fixation was indeed more beneficial for biomass build-up. Furthermore, elevated temperature significantly decreased $\tau_{ES}$ (Table 3, SI1), which can serves as a proxy of the rate

331  at which down-stream processes can remove electrons from PSII (Kolber et al., 1998). Thus,

332  our results indicate that the drainage of electrons into carbon fixation was faster under warmer

333  conditions, explaining the higher growth and biomass production under these conditions.

334

335  **4.2 Warming shifts CO$_2$ optima towards higher pCO$_2$ levels**

336  Under 6°C and pCO$_2$ levels expected to be reached by the end of this century, OA had a

337  significantly positive effect on growth and biomass build-up (Figure 1). This finding is in line

338  with previous studies, which have shown that picoeukaryotes can benefit strongly from OA in

339  both laboratory and mesocosm studies (Meakin and Wyman, 2011; Newbold et al., 2012;

340  Schaum et al., 2012; Brussaard et al., 2013; Maat et al., 2014; Schulz et al., 2017). Such positive

341  response to OA could indicate that picoeukaryotes such as *M. pusilla* are mainly dependent on

342  diffusive CO$_2$ supply and thus directly benefit from higher CO$_2$ concentrations (Brussaard et

343  al., 2013; Schulz et al., 2013; Schulz et al., 2017). While this could be related to the large surface

344  to volume ratio of small cells, opposite trends within the group of diatoms (i.e. higher sensitivity

345  of larger compared to smaller diatoms; Wu et al.; 2014; Sett et al. 2018) suggest more complex

346  underlying mechanisms at play.

347      Despite this overall effect, growth rates of *M. pusilla* tended to follow a non-linear

348  response curve over the tested range of glacial to elevated future pCO$_2$ levels (i.e. 180 to 1400

349  μatm), i.e. growth increased with increasing pCO$_2$ from low to intermediate, but decreased

350  again under the highest pCO$_2$ levels (Figure 1). Such an optimum behaviour can be expected

351  for most environmental drivers (Harley et al., 2017) and has previously been observed in

352  response to OA (Sett et al., 2014; Wolf et al., 2018; Hoppe et al. 2018). The response patterns

353  in these studies were attributed to a combination of beneficial effects of rising pCO$_2$ under

354  potentially carbon-limiting conditions for photosynthesis, and negative effects of declining pH

355  on cellular homeostasis and enzyme performance, which manifest mainly at high pCO$_2$ (Bach

356  et al., 2013). This non-linearity in the observed pCO$_2$ effects emphasises the importance of

357  experiments with more than two pCO$_2$ levels in order to properly describe OA-response patterns

358  of organisms.

359      On a more general level, apparent discrepancies between OA studies can be attributed

360  to actual differences in the environmental settings and their interactive effects with pCO$_2$

361  (Riebesell and Gattuso, 2015). When comparing the two most commonly applied pCO$_2$ levels,

362  i.e. the present-day and the anticipated end-of-century situation, the effects of OA on most of

363  the investigated physiological parameters are reversed under 6°C compared to 2°C (Figure 3).

364  This illustrates how difficult it is to infer responses to OA from experiments applying only one

set of environmental conditions. It is also noteworthy that the combination of OA and warming led to more densely packed cells (no change in cell size based on flow cytometric measurements; data not shown) with similar stoichiometry compared to the control treatment (Table 2). This indicates that cells managed to cope well with the experienced future conditions. Furthermore, warming altered the OA-dependent change in most of the investigated parameters in a direction that indicates higher fitness compared to low temperatures (e.g. higher growth rates and higher elemental quota; Figure 3). Thus, the increase in growth under future compared to ambient conditions was larger than what would be expected by the respective responses to warming and OA in isolation, indicating synergistic beneficial effects of both drivers.

**4.3 Potential mechanism underlying the interaction between warming and OA**

The observed synergistic effects could be explained by their specific impacts on carbon acquisition and fixation. As outlined in the introduction, light and dark reaction of photosynthesis need to be balanced to achieve high biomass production while avoiding photodamage (Behrenfeld et al., 2008). According to our data, this balance is shifted towards higher biomass production rates under warming and OA.

At higher temperatures, seawater $CO_2$ concentrations were lower than under colder conditions (Table 1; Zeebe and Wolf-Gladrow, 2001). At the same time, warming from 2°C to 6°C caused up to 60% higher growth and 110% higher biomass build-up rates (Figure 1, Table 2). Furthermore, the decrease in $\tau_{ES}$ indicates a faster transfer of photochemical energy into downstream processes such as RuBisCO activity (Table 3). Increased carbon demand in concert with lower carbon supply at higher temperatures thus increases the risk of $CO_2$ shortage in the cell, which in turn causes OA to have larger effects than at colder temperatures. Moreover, warming changes the kinetics of carbon fixation, with RuBisCO increasing its maximum turnover rates but decreasing its affinity for $CO_2$ (Young et al., 2014). At higher temperature, cells thus have the potential for higher carboxylation rates provided sufficient $CO_2$ is available (Kranz et al., 2015). Under elevated $pCO_2$ levels, diffusive $CO_2$ supply increases and/or costs for active carbon acquisition decrease. Consequently, the positive effect of increasing temperature on the carbon fixation rate can develop its full potential under OA.

In conclusion, elevated catabolic activity under warmer conditions can explain the observed upward shift in the $CO_2$-optimum of growth with increasing temperature (Figure 1), as the corresponding higher carbon demand causes $CO_2$ fixation to saturate under higher $pCO_2$ levels. In combination with a faster and more efficient machinery for pH homeostasis at elevated temperatures (Morgan-Kiss et al., 2006), this could explain why declining growth rates

399  were only observed at relatively higher $pCO_2$ levels compared to those under low temperature

400  conditions (Figure 2).

**4.4 Implications for the current and future Arctic pelagic ecosystem**

Picoeukaryotes such as *M. pusilla* are considered to be potential winners of climate change: They are not only thriving in warmer, more stratified environments, which are predicted to further expand in the future, but also seem to benefit from OA (Li et al., 2009; Schulz et al., 2017). Our results for *M. pusilla* confirm beneficial effects of warming and OA on growth and biomass production under nutrient-replete conditions (Figure 1, Table 2). Hence, in warmer spring conditions of the future, this species may experience growth stimulation under OA, potentially increasing its importance early in the growing season. Currently, *M. pusilla* already dominates Arctic phytoplankton assemblages in the nutrient-limited summer and autumn situations, which were not investigated in this study. Regarding the importance of nutrient availability, laboratory experiments found beneficial OA effects on *M. pusilla* primary production to persist also under P limitation (Maat et al., 2014), while in a mesocosm community, OA-dependent increases in *M. pusilla* abundances disappeared when the system ran into P and N co-limitation (Engel et al., 2008). Thus, it remains to be seen how the combined effects of warming and OA manifest under low nutrient conditions as well as how the responses may depend on sources and types of nutrients (e.g. mixing-delivered nitrate vs. regenerated ammonium).

A species' success in the environment does not only depend on individual performance, but also on how it compares to that of competing species. When we compare our results with the responses of the Arctic diatom *Thalassiosira hyalina*, isolated from the same location and exposed to the same experimental conditions (Wolf et al., 2018), the diatom had higher growth rates than the picoeukaryote under most treatment conditions, as can be expected for nutrient-replete conditions (Sarthou et al., 2005). The relative increase in growth rates from ambient (2 or 3°C and 380 µatm $pCO_2$) to future conditions (6°C and 1000 µatm $pCO_2$) was, however, much higher for *M. pusilla* than for *T. hyalina*. The fact that our experiments were conducted under nutrient-replete conditions, which typically favour diatoms over picoeukaryotes, may indicate an even stronger increase in fitness (Collins et al., 2014) and could mean that *M. pusilla* gains another competitive advantage over phytoplankton like diatoms in the future, in addition to those resulting from changes in stratification (Li et al., 2009). Thus, our findings suggest higher picoplankton contribution to future Arctic phytoplankton assemblages under non-limiting conditions, e.g. early in the growing season when picoeukaryotes can already contribute quite substantially to the phytoplankton standing stocks (Marquardt et al, 2017, Paulsen et al. 2015). How such competition between diatoms and picoeukaryotes would

434  manifest under nutrient-depleted conditions that strongly favour *M. pusilla* is currently
435  unknown.

436      Even though picoeukaryotes seem to contribute more to the downward export of organic
437  matter than previously assumed (Waite et al., 2000; Richardson and Jackson, 2007), in
438  comparison to e.g. diatoms, they are less efficient vectors for carbon export to depth and have
439  a lower energy transfer along trophic levels (Sherr et al., 2003). Consequently, Arctic food webs
440  dominated by picoeukaryotes would look very different from those fuelled by diatom
441  production (Sherr et al., 2003; Paulsen et al., 2015). Due to its motility and capability to grow
442  mixotrophically, *M. pusilla* is characterized by an exceptionally high cellular C:N ratio
443  compared to other Arctic phytoplankton (Table 2; Halsey et al., 2014; McKie-Krisberg and
444  Sanders, 2014). An increased importance of this species would thus not only affect the food
445  web due to its small size and concurrent grazer preferences, but also in terms of food quality
446  (van de Waal and Boersma, 2012). The expected higher growth rates and thus abundances of
447  this species may thus strengthen the Arctic microbial food web. Together with a concurrent
448  weakening of the classical diatom-fuelled food web, this could have severe implications for the
449  flow of energy and nutrients through future marine Arctic ecosystems (Post, 2016).

450

451  **4.5 Conclusions**
452  This study is the first to show synergistic effects of warming and OA on *M. pusilla*, one of the
453  most abundant species of the worlds' oceans. Individually, both warming and OA cause more
454  efficient biomass build-up under nutrient-replete conditions. Beneficial effects manifest,
455  however, even more strongly in combination, when facilitated carbon acquisition (e.g. due to
456  higher diffusive $CO_2$ supply) co-occurs with higher fixation rates (e.g. due to higher turnover-
457  rates of RuBisCO). Our results provide an explanation for the observations of previous
458  mesocosm studies, which indicated beneficial effects of OA and warming on *M. pusilla* and
459  other picoeukaryotes. Characterising the responses of this Arctic key species to warming and
460  OA will help to develop mechanistic phytoplankton functional types and more realistic model
461  representation of phytoplankton assemblages as well as their responses to multiple drivers.
462  Future studies are needed to elucidate further multifactorial environmental changes, addressing
463  both abiotic (e.g. changes in light and nutrients) as well as biotic (e.g. heterotrophy,
464  competition, grazers, viruses) interactions.

**Author Contributions**

C.J.M.H. and B.R. designed the study. C.J.M.H. and C.F. conducted the experiment. C.J.M.H. analysed the data and prepared the manuscript with contributions from B.R. and C.F.

The authors declare that they have no conflict of interest.

**Acknowledgements**

We are grateful for field support by the 2014/15 station team of the AWIPEV base in Ny-Ålesund (Svalbard) as well as K. Wolf's help with strain isolation and maintenance of *M. pusilla* cultures. We thank U. John and N. Kühne for sequencing and help with the molecular strain identification. Furthermore, L. Wischnewski, A. Terbrüggen and M. Machnik are acknowledged for their help with sample analyses.

# References

AMAP: AMAP Assessment 2013: Arctic Ocean Acidification, Arctic Monitoring and Assessment Programme (AMAP), Oslo, Norway, 99, 2013.

Arrigo, K. R., van Dijken, G., and Pabi, S.: Impact of a shrinking Arctic ice cover on marine primary production, Geophysical Research Letters, 35, L19603, 10.1029/2008gl035028, 2008.

Bach, L. T., Mackinder, L. C. M., Schulz, K. G., Wheeler, G., Schroeder, D. C., Brownlee, C., and Riebesell, U.: Dissecting the impact of $CO_2$ and pH on the mechanisms of photosynthesis and calcification in the coccolithophore Emiliania huxleyi, New Phytologist, n/a-n/a, 10.1111/nph.12225, 2013.

Behrenfeld, M. J., Halsey, K. H., and Milligan, A. J.: Evolved physiological responses of phytoplankton to their integrated growth environment, Philosophical Transactions of the Royal Society B: Biological Sciences, 363, 2687-2703, 10.1098/rstb.2008.0019, 2008.

Berge, J., Daase, M., Renaud, Paul E., Ambrose, William G., Jr., Darnis, G., Last, Kim S., Leu, E., Cohen, Jonathan H., Johnsen, G., Moline, Mark A., Cottier, F., Varpe, Ø., Shunatova, N., Bałazy, P., Morata, N., Massabuau, J.-C., Falk-Petersen, S., Kosobokova, K., Hoppe, Clara J. M., Węsławski, Jan M., Kukliński, P., Legeżyńska, J., Nikishina, D., Cusa, M., Kędra, M., Włodarska-Kowalczuk, M., Vogedes, D., Camus, L., Tran, D., Michaud, E., Gabrielsen, Tove M., Granovitch, A., Gonchar, A., Krapp, R., and Callesen, Trine A.: Unexpected Levels of Biological Activity during the Polar Night Offer New Perspectives on a Warming Arctic, Curr. Biol., 25, 2555-2561, 10.1016/j.cub.2015.08.024, 2015.

Brewer, P. G., Bradshaw, A. L., and Williams, R. T.: Measurement of total carbon dioxide and alkalinity in the North Atlantic ocean in 1981, in: The Changing Carbon Cycle – A Global Analysis edited by: Trabalka, J. R., and Reichle, D. E., Springer Verlag, Heidelberg Berlin, 358–381, 1986.

Brown, J. H., Gillooly, J. F., Allen, A. P., Savage, V. M., and West, G. B.: Toward a metabolic theorie of ecology, Ecology, 85, 1771-1789, 10.1890/03-9000, 2004.

Brussaard, C. P. D., Noordeloos, A. A. M., Witte, H., Collenteur, M. C. J., Schulz, K., Ludwig, A., and Riebesell, U.: Arctic microbial community dynamics influenced by elevated $CO_2$ levels, Biogeosciences, 10, 719-731, 10.5194/bg-10-719-2013, 2013.

Collins, M., Knutti, R., Arblaster, J., Dufresne, J.-L., Fichefet, T., Friedlingstein, P., Gao, X., Gutowski, W., Johns, T., and Krinner, G.: Long-term climate change: projections, commitments and irreversibility, 2013.

Collins, S., Rost, B., and Rynearson, T. A.: Evolutionary potential of marine phytoplankton under ocean acidification, Evolutionary Applications, 7, 140-155, 10.1111/eva.12120, 2014.

Daufresne, M., Lengfellner, K., and Sommer, U.: Global warming benefits the small in aquatic ecosystems, Proceedings of the National Academy of Sciences, 106, 12788-12793, 10.1073/pnas.0902080106, 2009.

Dickson, A. G., and Millero, F. J.: A comparison of the equilibrium constants for the dissociation of carbonic acid in seawater media, Deep-Sea Research, 34, 1733– 1743, 1987.

Dickson, A. G.: Standard potential of the reaction: AgCl(s) + ½ H2(g) = Ag(s) + HCl(aq), and the standard acidity constant of the ion $HSO_4^-$ in synthetic seawater from 273.15 to 318.15 K, Journal of Chemical Thermodynamics, 22, 113-127, 10.1016/0021-9614(90)90074-Z, 1990.

Dickson, A. G., Sabine, C. L., and Christian, J. R.: Guide to best practices for ocean $CO_2$ measurements, North Pacific Marine Science Organization, Sidney, British Columbia, 191, 2007.

Engel, A., Schulz, K. G., Riebesell, U., Bellerby, R., Delille, B., and Schartau, M.: Effects of $CO_2$ on particle size distribution and phytoplankton abundance during a mesocosm bloom experiment (PeECE II), Biogeosciences, 5, 509-521, 10.5194/bg-5-509-2008, 2008.

Eppley, R. W.: Temperature and phytoplankton growth in the sea, Fish. Bull, 70, 1063-1085, 1972.

Flynn, K. J., Blackford, J. C., Baird, M. E., Raven, J. A., Clark, D. R., Beardall, J., Brownlee, C., Fabian, H., and Wheeler, G. L.: Changes in pH at the exterior surface of plankton with ocean acidification, Nature Clim. Change, 2, 510-513, 2012.

Genty, B., Briantais, J.-M., and Baker, N. R.: The relationship between the quantum yield of photosynthetic electron transport and quenching of chlorophyll fluorescence, Biochimica et Biophysica Acta (BBA) - General Subjects, 990, 87-92, 10.1016/s0304-4165(89)80016-9, 1989.

Guillard, R. R. L., and Ryther, J. H.: Studies of marine planktonic diatoms. I. Cyclothella nana Hustedt and  Detonula confervacea Cleve Can. J. Microbiol., 8, 229-239, 1962.

Halsey, K., Milligan, A., and Behrenfeld, M.: Contrasting Strategies of Photosynthetic Energy Utilization Drive Lifestyle Strategies in Ecologically Important Picoeukaryotes, Metabolites, 4, 260-280, 2014.

Halsey, K. H., and Jones, B. M.: Phytoplankton Strategies for Photosynthetic Energy Allocation, Annual Review of Marine Science, 7, 265-297, doi:10.1146/annurev-marine-010814-015813, 2015.

Harley, C. D. G., Connell, S. D., Doubleday, Z. A., Kelaher, B., Russell, B. D., Sarà, G., and Helmuth, B.: Conceptualizing ecosystem tipping points within a physiological framework, Ecology and Evolution, 10.1002/ece3.3164, 2017.

Hegseth, E. N., Assmy, P., Wiktor, J., Kristiansen, S., Leu, E., Tverberg, V., Gabrielsen, G. W., Skogseth, R., and Cottier, F. R.: Phytoplankton seasonal dynamics in Kongsfjorden,

Svalbard and the adjacent shelf, in: The Ecosystem of Kongsfjorden, Svalbard, edited by: Hop, H., and Wiencke, C., Springer, in press.

Hoppe, C. J. M., Langer, G., Rokitta, S. D., Wolf-Gladrow, D. A., and Rost, B.: Implications of observed inconsistencies in carbonate chemistry measurements for ocean acidification studies, Biogeosciences, 9, 2401–2405, 10.5194/bg-9-2401-2012, 2012.

Hoppe, C. J. M., Holtz, L.-M., Trimborn, S., and Rost, B.: Ocean acidification decreases the light-use efficiency in an Antarctic diatom under dynamic but not constant light, New Phytologist, 207, 159-171, 10.1111/nph.13334, 2015.

Hoppe, C. J. M., Wolf, K. K. E., Schuback, N., Tortell, P. D., and Rost, B.: Compensation of ocean acidification effects in Arctic phytoplankton assemblages, Nature Climate Change, 8, 529–533, 1038/s41558-018-0142-9, 2018.

Hussherr, R., Levasseur, M., Lizotte, M., Tremblay, J. É., Mol, J., Thomas, H., Gosselin, M., Starr, M., Miller, L. A., Jarniková, T., Schuback, N., and Mucci, A.: Impact of ocean acidification on Arctic phytoplankton blooms and dimethyl sulfide concentration under simulated ice-free and under-ice conditions, Biogeosciences, 14, 2407-2427, 10.5194/bg-14-2407-2017, 2017.

Knap, A., Michaels, A., Close, A., Ducklow, H., and Dickson, A..: Protocols for the Joint Global Ocean Flux Study (JGOFS) Core Measurements., UNESCO, 170, 1996.

Kolber, Z. S., Prasil, O., and Falkowski, P. G.: Measurements of variable chlorophyll fluorescence using fast repetition rate techniques. I. Defining methodology and experimental protocols, Biochem. Biophys. Acta, 1367, 88-106, 1998.

Kranz, S. A., Young, J. N., Hopkinson, B. M., Goldman, J. A. L., Tortell, P. D., and Morel, F. M. M.: Low temperature reduces the energetic requirement for the $CO_2$ concentrating mechanism in diatoms, New Phytologist, 205, 192-201, 10.1111/nph.12976, 2015.

Levitt, J.: Responses of Plants to Environmental Stress, Volume 1: Chilling, Freezing, and High Temperature Stresses, Academic Press., 1980.

Li, W. K. W., McLaughlin, F. A., Lovejoy, C., and Carmack, E. C.: Smallest Algae Thrive As the Arctic Ocean Freshens, Science, 326, 539, 10.1126/science.1179798, 2009.

Lovejoy, C., Vincent, W. F., Bonilla, S., Roy, S., Martineau, M.-J., Terrado, R., Potvin, M., Massana, R., and Pedrós-Alió, C.: Distribution, phylogeny, and growth of cold-adapted picoprasinophytes in Arctic Seas, Journal of Phycology, 43, 78-89, 10.1111/j.1529-8817.2006.00310.x, 2007.

Lovejoy, C.: Changing Views of Arctic Protists (Marine Microbial Eukaryotes) in a Changing Arctic, Acta Protozool., 53, 91-100, 10.4467/16890027ap.14.009.1446, 2014.

Maat, D. S., Crawfurd, K. J., Timmermans, K. R., and Brussaard, C. P. D.: Elevated $CO_2$ and Phosphate Limitation Favor Micromonas pusilla through Stimulated Growth and Reduced

Viral Impact, Applied and Environmental Microbiology, 80, 3119-3127, 10.1128/aem.03639-13, 2014.

Marquardt, M., Vader, A., Stübner, E. I., Reigstad, M., and Gabrielsen, T. M.: Strong Seasonality of Marine Microbial Eukaryotes in a High-Arctic Fjord (Isfjorden, in West Spitsbergen, Norway), Applied and Environmental Microbiology, 82, 1868-1880, 10.1128/aem.03208-15, 2016.

Maxwell, D. P., Falk, S., Trick, C. G., and Huner, N.: Growth at Low Temperature Mimics High-Light Acclimation in Chlorella vulgaris, Plant Physiology, 105, 535-543, 10.1104/pp.105.2.535, 1994.

Maxwell, K., and Johnson, G. N.: Chlorophyll fluorescence a practical guide, J. Exp. Bot., 51, 659-668, 10.1093/jexbot/51.345.659, 2000.

McKew, B. A., Davey, P., Finch, S. J., Hopkins, J., Lefebvre, S. C., Metodiev, M. V., Oxborough, K., Raines, C. A., Lawson, T., and Geider, R. J.: The trade-off between the light-harvesting and photoprotective functions of fucoxanthin-chlorophyll proteins dominates light acclimation in *Emiliania huxleyi* (clone CCMP 1516), New Phytologist, 200, 74-85, 10.1111/nph.12373, 2013.

McKie-Krisberg, Z. M., and Sanders, R. W.: Phagotrophy by the picoeukaryotic green alga *Micromonas*: implications for Arctic Oceans, ISME J, 8, 1953-1961, 10.1038/ismej.2014.16, 2014.

Meakin, N. G., and Wyman, M.: Rapid shifts in picoeukaryote community structure in response to ocean acidification, ISME J, 5, 1397-1405, 2011.

Mehrbach, C., Culberson, C. H., Hawley, J. E., and Pytkowicz, R. M.: Measurement of the apparent dissociation constants of carbonic acid in seawater at atmospheric pressure, Limnology and Oceanography, 18, 897–907, 10.4319/lo.1973.18.6.0897, 1973.

Miller, G. H., Alley, R. B., Brigham-Grette, J., Fitzpatrick, J. J., Polyak, L., Serreze, M. C., and White, J. W. C.: Arctic amplification: can the past constrain the future?, Quaternary Science Reviews, 29, 1779-1790, 10.1016/j.quascirev.2010.02.008, 2010.

Mock, T., and Hoch, N.: Long-Term Temperature Acclimation of Photosynthesis in Steady-State Cultures of the Polar Diatom *Fragilariopsis cylindrus*, Photosynth Res, 85, 307-317, 10.1007/s11120-005-5668-9, 2005.

Morgan-Kiss, R. M., Priscu, J. C., Pocock, T., Gudynaite-Savitch, L., and Huner, N. P. A.: Adaptation and Acclimation of Photosynthetic Microorganisms to Permanently Cold Environments, Microbiology and Molecular Biology Reviews, 70, 222-252, 10.1128/mmbr.70.1.222-252.2006, 2006.

Newbold, L. K., Oliver, A. E., Booth, T., Tiwari, B., DeSantis, T., Maguire, M., Andersen, G., van der Gast, C. J., and Whiteley, A. S.: The response of marine picoplankton to ocean

acidification, Environmental Microbiology, 14, 2293-2307, 10.1111/j.1462-2920.2012.02762.x, 2012.

Oxborough, K.: FastPro8 GUI and FRRf3 systems documentation. Chelsea Technologies Group Ltd 2012, 2012.

Paulsen, M. L., Riisgaard, K., Frede, T., St John, M., and Nielsen, T. G.: Winter− spring transition in the subarcticAtlantic: microbial response to deep mixingand pre-bloom production, 2015.

Pierrot, D. E., Lewis, E., and Wallace, D. W. R.: MS Exel Program Developed for CO2 System Calculations. ORNL/CDIAC-105aCarbon Dioxide Information Analysis Centre, O. R. N. L. (Ed.), US Department of Energy, Oak Ridge, Tennessee, 2006.

Post, E.: Implications of earlier sea ice melt for phenological cascades in arctic marine food webs, Food Webs, 10.1016/j.fooweb.2016.11.002, 2016.

Qi, D., Chen, L., Chen, B., Gao, Z., Zhong, W., Feely, R. A., Anderson, L. G., Sun, H., Chen, J., Chen, M., Zhan, L., Zhang, Y., and Cai, W.-J.: Increase in acidifying water in the western Arctic Ocean, Nature Clim. Change, 7, 195-199, 10.1038/nclimate3228, 2017.

Raven, J.: The twelfth Tansley Lecture. Small is beautiful: the picophytoplankton, Funct. Ecol., 12, 503-513, 1998.

Richardson, T. L., and Jackson, G. A.: Small Phytoplankton and Carbon Export from the Surface Ocean, Science, 315, 838-840, 10.1126/science.1133471, 2007.

Riebesell, U., and Gattuso, J.-P.: Lessons learned from ocean acidification research, Nature Climate Change, 5, 12-14, 2015.

Rost, B., Zondervan, I., and Wolf-Gladrow, D.: Sensitivity of phytoplankton to future changes in ocean carbonate chemistry: Current knowledge, contradictions and research needs, Mar. Ecol. Prog. Ser., 373, 227-237, 10.3354/meps07776, 2008.

Sarthou, G., Timmermans, K. R., Blain, S., and Tréguer, P.: Growth physiology and fate of diatoms in the ocean: a review, J. Sea Res., 53, 25-42, 10.1016/j.seares.2004.01.007, 2005.

Schaum, E., Rost, B., Millar, A. J., and Collins, S.: Variation in plastic responses of a globally distributed picoplankton species to ocean acidification, Nature Climate Change, 3, 298–302, 10.1038/nclimate1774, 2012.

Schulz, K. G., Bellerby, R. G. J., Brussaard, C. P. D., Büdenbender, J., Czerny, J., Engel, A., Fischer, M., Koch-Klavsen, S., Krug, S. A., Lischka, S., Ludwig, A., Meyerhöfer, M., Nondal, G., Silyakova, A., Stuhr, A., and Riebesell, U.: Temporal biomass dynamics of an Arctic plankton bloom in response to increasing levels of atmospheric carbon dioxide, Biogeosciences, 10, 161  - 180, 10.5194/bg-10-161-2013, 2013.

Schulz, K. G., Bach, L. T., Bellerby, R. G. J., Bermúdez, R., Büdenbender, J., Boxhammer, T., Czerny, J., Engel, A., Ludwig, A., Meyerhöfer, M., Larsen, A., Paul, A. J., Sswat, M., and Riebesell, U.: Phytoplankton Blooms at Increasing Levels of Atmospheric Carbon Dioxide: Experimental Evidence for Negative Effects on Prymnesiophytes and Positive on Small Picoeukaryotes, Frontiers in Marine Science, 4, 10.3389/fmars.2017.00064, 2017.

Sett, S., Schulz, K. G., Bach, L. T., and Riebesell, U.: Shift towards larger diatoms in a natural phytoplankton assemblage under combined high-$CO_2$ and warming conditions, J. Plankton Res., 10.1093/plankt/fby018, 2018.

Sett, S., Bach, L. T., Schulz, K. G., Koch-Klavsen, S., Lebrato, M., and Riebesell, U.: Temperature Modulates Coccolithophorid Sensitivity of Growth, Photosynthesis and Calcification to Increasing Seawater $pCO_2$, PLoS ONE, 9, e88308, 10.1371/journal.pone.0088308, 2014.

Sherr, E. B., and Sherr, B. F.: Significance of predation by protists in aquatic microbial food webs, Antonie Leeuwenhoek, 81, 293-308, 10.1023/a:1020591307260, 2002.

Sherr, E. B., Sherr, B. F., Wheeler, P. A., and Thompson, K.: Temporal and spatial variation in stocks of autotrophic and heterotrophic microbes in the upper water column of the central Arctic Ocean, Deep Sea Research Part I: Oceanographic Research Papers, 50, 557-571, 10.1016/S0967-0637(03)00031-1, 2003.

Silsbe, G. M., and Kromkamp, J. C.: Modeling the irradiance dependency of the quantum efficiency of photosynthesis, Limnol. Oceanogr. Methods, 10, 645-652, 2012.

Šlapeta, J., López-García, P. n., and Moreira, D.: Global Dispersal and Ancient Cryptic Species in the Smallest Marine Eukaryotes, Mol. Biol. Evol., 23, 23-29, 10.1093/molbev/msj001, 2006.

Sommer, U., Paul, C., and Moustaka-Gouni, M.: Warming and ocean acidification effects on phytoplankton—from species shifts to size shifts within species in a mesocosm experiment, PLoS One, 10, e0125239, 2015.

Stocker, T.: Climate change 2013: the physical science basis: Working Group I contribution to the Fifth assessment report of the Intergovernmental Panel on Climate Change, Cambridge University Press, 2014.

Stoll, M. H. C., Bakker, K., Nobbe, G. H., and Haese, R. R.: Continous-Flow Analysis of Dissolved Inorganic Carbon Content in Seawater, Analytical Chemistry, 73, 4111-4116, 2001.

Suggett, D. J., Borowitzka, M. A., and Prášil, O. E.: Chlorophyll a Fluorescence in Aquatic Sciences: Methods and Applications, Developments in Applied Phycology, Springer, Dordrecht, 326 pp., 2010.

Taylor, A. R., Chrachri, A., Wheeler, G., Goddard, H., and Brownlee, C.: A Voltage-Gated $H^+$ Channel Underlying pH Homeostasis in Calcifying Coccolithophores, PLoS Biol., 9, 10.1371/journal.pbio.1001085, 2001.

Toseland, A., Daines, S. J., Clark, J. R., Kirkham, A., Strauss, J., Uhlig, C., Lenton, T. M., Valentin, K., Pearson, G. A., Moulton, V., and Mock, T.: The impact of temperature on marine phytoplankton resource allocation and metabolism, Nature Clim. Change, 3, 979-984, 10.1038/nclimate1989, 2013.

Tremblay, G., Belzile, C., Gosselin, M., Poulin, M., Roy, S., and Tremblay, J. E.: Late summer phytoplankton distribution along a 3500 km transect in Canadian Arctic waters: strong numerical dominance by picoeukaryotes, Aquat. Microb. Ecol., 54, 55-70, 2009.

Tremblay, J.-É., Anderson, L. G., Matrai, P., Coupel, P., Bélanger, S., Michel, C., and Reigstad, M.: Global and regional drivers of nutrient supply, primary production and $CO_2$ drawdown in the changing Arctic Ocean, Progress in Oceanography, 139, 171-196, 10.1016/j.pocean.2015.08.009, 2015.

Vader, A., Marquardt, M., Meshram, A. R., and Gabrielsen, T. M.: Key Arctic phototrophs are widespread in the polar night, Polar Biol, 38, 13-21, 10.1007/s00300-014-1570-2, 2015.

van de Waal, D., and Boersma, M.: Ecological stoichiometry in aquatic ecosystems, in: Encyclopedia of Life Support Systems (EOLSS), Developed under the Auspices of the UNESCO (eds. UNESCO-EOLSS Joint Committee), Eolss Publishers, 2012.

Waite, A. M., Safi, K. A., Hall, J. A., and Nodder, S. D.: Mass sedimentation of picoplankton embedded in organic aggregates, Limnology and Oceanography, 45, 87-97, 10.4319/lo.2000.45.1.0087, 2000.

Wassmann, P., and Reigstad, M.: Future Arctic Ocean seasonal ice zones and implications for pelagic-benthic coupling, Oceanography, 24, 220-231, 10.5670/oceanog.2011.74., 2011.

Webb, W., Newton, M., and Starr, D.: Carbon dioxide exchange of *Alnus rubra*, Oecologia, 17, 281-291, 10.1007/bf00345747, 1974.

Wolf, K., Hoppe, C. J. M., and Rost, B.: Resilience by diversity: Large intraspecific differences in climate change responses of an Arctic diatom, Limnology and Oceanography, 63, 397-411, 10.1002/lno.10639, 2018.

Worden, A. Z., and Not, F.: Ecology and diversity of picoeukaryotes, Microbial Ecology of the Oceans, Second Edition, 159-205, 2008.

Worden, A. Z., Follows, M. J., Giovannoni, S. J., Wilken, S., Zimmerman, A. E., and Keeling, P. J.: Rethinking the marine carbon cycle: Factoring in the multifarious lifestyles of microbes, Science, 347, 10.1126/science.1257594, 2015.

Wu, Y., Campbell, D. A., Irwin, A. J., Suggett, D. J., and Finkel, Z. V.: Ocean acidification

enhances the growth rate of larger diatoms, Limnology and Oceanography, 59, 1027-1034, 10.4319/lo.2014.59.3.1027, 2014.

Young, J. N., Goldman, J. A. L., Kranz, S. A., Tortell, P. D., and Morel, F. M. M.: Slow carboxylation of Rubisco constrains the rate of carbon fixation during Antarctic phytoplankton blooms, New Phytologist, 205, 172–181, 10.1111/nph.13021, 2014.

Zeebe, R. E., and Wolf-Gladrow, D. A.: $CO_2$ in Seawater: Equilibrium, Kinetics, Isotopes, Elsevier Science, Amsterdam, 2001.

Table 1: Seawater carbonate chemistry at the end of the experiments (n=3; mean ±1 s.d.). $CO_2$ partial pressure ($pCO_2$) and dissolved $CO_2$ concentrations were calculated from total alkalinity ($A_T$) and $pH_{total}$ at 2 or 6°C, a salinity of 32.7 using $CO_2SYS$ (Pierrot et al., 2006), and phosphate and silicate concentrations of 10 and 100 µmol $kg^{-1}$, respectively. n.a. indicates that values are not available for this specific treatment.

| Temperature [°C] | $pCO_2$ level [µatm] | pH total scale | $A_T$ [µmol $kg^{-1}$] | $C_T$ [µmol $kg^{-1}$] | dissolved $CO_2$ [µmol $kg^{-1}$] | $pCO_2$ [µatm] |
|---|---|---|---|---|---|---|
| 2 | 180 | 8.3 ± 0.01 | 2264 ± 9 | 2024 ± 6 | 11.6 ± 0.2 | 197 ± 3 |
| | 380 | 8.11 ± 0.01 | 2244 ± 30 | 2124 ± 11 | 19.0 ± 0.7 | 323 ± 12 |
| | 1000 | 7.68 ± 0.01 | 2255 ± 45 | 2215 ± 23 | 56.4 ± 1.3 | 959 ± 22 |
| | 1400 | 7.52 ± 0.02 | 2243 ± 5 | n.a. | 81.1 ± 3.1 | 1380 ± 53 |
| 6 | 180 | 8.3 ± 0.01 | 2243 ± 28 | 1969 ± 10 | 10.0 ± 0.3 | 198 ± 6 |
| | 380 | 8.04 ± 0.01 | 2256 ± 21 | 2058 ± 7 | 20.0 ± 0.5 | 394 ± 10 |
| | 1000 | 7.65 ± 0.01 | 2262 ± 22 | 2178 ± 14 | 52.6 ± 1.6 | 1036 ± 31 |
| | 1400 | 7.52 ± 0.01 | 2265 ± 5 | n.a. | 73.6 ± 0.9 | 1449 ± 18 |

Table 2: Growth rate constants $\mu$, division rate constants $k$, POC production rates and cellular quota of Chl *a*, POC and PON as well as their ratios of *M. pusilla* at the end of the experiment under the different treatment conditions (n=3; mean ±1 s.d.). Results from statistical analysis can be found in Table SI2.

| Temperature [°C] | pCO$_2$ [µatm] | Growth rate constant μ [d$^{-1}$] | Division rate constant $k$ [d$^{-1}$] | POC production [fmol cell$^{-1}$ d$^{-1}$] | POC quota [fmol cell$^{-1}$] | PON quota [fmol cell$^{-1}$] | Chl a quota [fg cell$^{-1}$] | POC:PON [mol mol$^{-1}$] | POC:Chl *a* [g g$^{-1}$] |
|---|---|---|---|---|---|---|---|---|---|
| 2 | 180 | 0.75 ± 0.04 | 1.08 ± 0.05 | 256 ± 11 | 239 ± 20 | 28.7 ± 2.6 | 28.6 ± 2.1 | 8.3 ± 0.1 | 100 ± 7 |
|   | 380 | 0.85 ± 0.03 | 1.23 ± 0.04 | 290 ± 16 | 237 ± 22 | 30.9 ± 1.8 | 24.7 ± 1.4 | 7.7 ± 0.3 | 115 ± 10 |
|   | 1000 | 0.79 ± 0.05 | 1.15 ± 0.07 | 224 ± 23 | 196 ± 25 | 24.9 ± 4.9 | 20.0 ± 2.9 | 8.0 ± 0.6 | 118 ± 5 |
|   | 1400 | 0.82 ± 0.05 | 1.18 ± 0.07 | 235 ± 13 | 199 ± 16 | 23.9 ± 2.3 | 22.0 ± 1.5 | 8.4 ± 0.1 | 109 ± 4 |
| 6 | 180 | 1.06 ± 0.03 | 1.53 ± 0.05 | 376 ± 15 | 245 ± 3 | 26.9 ± 0.6 | 21.1 ± 0.8 | 9.1 ± 0.1 | 140 ± 7 |
|   | 380 | 1.05 ± 0.03 | 1.52 ± 0.04 | 342 ± 39 | 226 ± 26 | 25.9 ± 2.5 | 22.1 ± 2.6 | 8.7 ± 0.3 | 123 ± 11 |
|   | 1000 | 1.25 ± 0.05 | 1.80 ± 0.07 | 497 ± 12 | 275 ± 6 | 33.7 ± 2.0 | 27.2 ± 0.9 | 8.2 ± 0.6 | 122 ± 6 |
|   | 1400 | 1.05 ± 0.04 | 1.52 ± 0.06 | 400 ± 14 | 263 ± 7 | 31.1 ± 1.7 | 28.6 ± 3.2 | 8.5 ± 0.3 | 111 ± 16 |

Table 3: **:** FRR-flourometrical PSII photochemistry measurements – PSII quantum yield efficiency Fv/Fm [dimensionless], functional absorption cross section ($\sigma_{PSII}$) [nm$^{-2}$ PSII$^{-1}$]), rate of PSII re-opening ($\tau_{ES}$ [ms]), maximum non-photochemical quenching at 672 µmol photons m$^{-2}$ s$^{-1}$ (NPQ$_{max}$ [dimensionless]), maximum light-use efficiency (initial slope $\alpha$ [mol e$^{-}$ m$^2$ (mol RCII)$^{-1}$ (mol photons)$^{-1}$]), maximal absolute electron transfer rates through PSII (ETR$_{max}$ [mol e$^{-}$ (mol RCII)$^{-1}$ s$^{-1}$]), and the light saturation index (E$_K$ [µmol photons m$^{-2}$ s$^{-1}$]) under the different temperature and pCO$_2$ treatments (n=3; mean ±1 s.d.). Results from statistical analysis can be found in Table SI2.

| Temp | pCO$_2$ | Fv/Fm | $\sigma_{PSII}$ | $\tau_{ES}$ | NPQ$_{max}$ | $\alpha$ | ETR$_{max}$ | E$_K$ |
|---|---|---|---|---|---|---|---|---|
| 2 | 180 | 0.50 ± 0.01 | 8.66 ± 0.35 | 439 ± 8 | 2.26 ± 0.18 | 0.42 ± 0.05 | 33 ± 2 | 81 ± 13 |
| | 380 | 0.43 ± 0.09 | 8.93 ± 0.26 | 425 ± 4 | 3.51 ± 0.55 | 0.32 ± 0.15 | 25 ± 5 | 91 ± 44 |
| | 1000 | 0.45 ± 0.08 | 8.55 ± 0.07 | 448 ± 1 | 3.96 ± 0.71 | 0.42 ± 0.03 | 31 ± 2 | 75 ± 10 |
| | 1400 | 0.47 ± 0.10 | 9.06 ± 0.05 | 422 ± 14 | 2.45 ± 0.44 | 0.43 ± 0.08 | 31 ± 7 | 75 ± 31 |
| 6 | 180 | 0.49 ± 0.01 | 9.22 ± 0.22 | 412 ± 6 | 2.51 ± 0.37 | 0.49 ± 0.08 | 28 ± 10 | 59 ± 28 |
| | 380 | 0.43 ± 0.12 | 8.83 ± 0.17 | 427 ± 6 | 2.83 ± 0.59 | 0.38 ± 0.09 | 35 ± 14 | 90 ± 17 |
| | 1000 | 0.41 ± 0.07 | 8.91 ± 0.22 | 422 ± 11 | 4.94 ± 1.46 | 0.33 ± 0.09 | 32 ± 5 | 100 ± 21 |
| | 1400 | 0.45 ± 0.04 | 8.71 ± 0.50 | 428 ± 19 | 2.93 ± 0.50 | 0.38 ± 0.04 | 40 ± 5 | 104 ± 6 |

Figure 1: Specific growth rate constant μ (A) and POC production (B) of *M. pusilla* under low (filled symbols) and high temperatures (open symbols) as a function of $pCO_2$ (n=3; mean ±1 s.d.). Results from statistical analysis can be found in Table SI2.
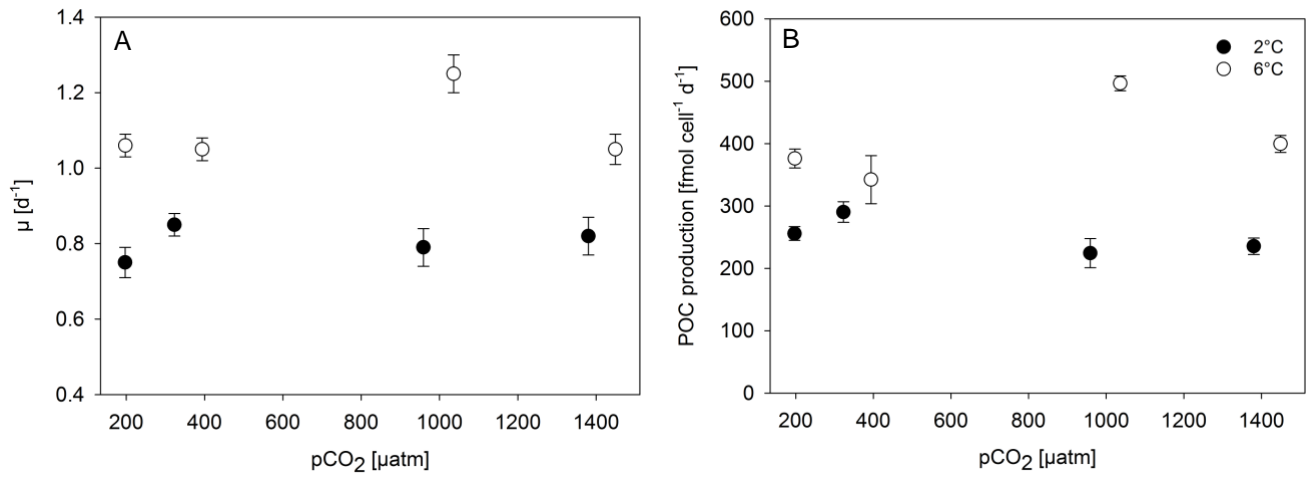
Figure 2: Cellular composition, i.e. POC (A), PON (B) and Chl *a* quota (C) as well as as C:Chl *a* ratios (D), of *M. pusilla* under low (filled symbols) and high temperatures (open symbols) as a function of pCO$_2$ ( n=3; mean ±1 s.d.). Results from statistical analysis can be found in Table SI2.
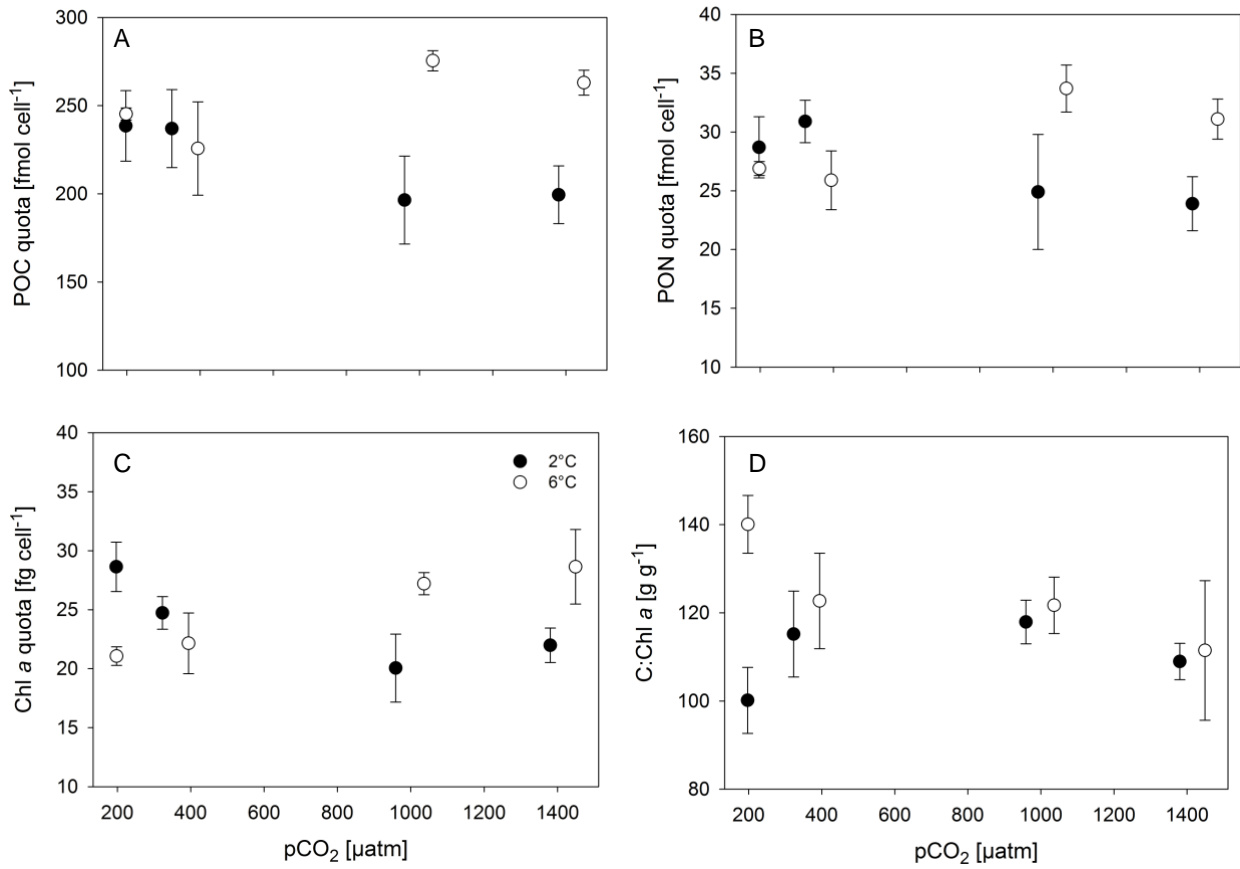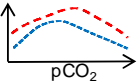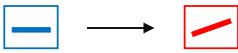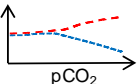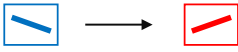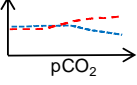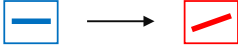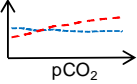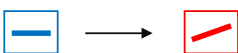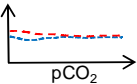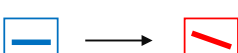
Figure 3: Schematic illustration of results for both temperatures over the entire range of $pCO_2$ levels as well as focusing on the responses between 380 and 1000 µatm (as the representation for commonly used OA treatments) and their modulation by temperature.

| Parameter | Response curves | 380 - 1000 µatm effect 2°C → 6°C | | |
|---|---|---|---|---|
| Growth | | | → | |
| POC quota | | | → | |
| PON quota | | | → | |
| Chl *a* quota | | | → | |
| C:N | | | → | |
| C:Chla | | | → | |